



Carbon Reinforced Concrete Members Under Concentrated Load

Jan Philip Schulze-Ardey^(✉), Sven Bosbach, Ann-Christine von der Heid,
and Josef Hegger

Institute of Structural Concrete, RWTH Aachen University, 52074 Aachen, Germany
jschulze@imb.rwth-aachen.de

Abstract. Many buildings are already realized with elements made of textile reinforced concrete. This innovative composite material offers numerous advantages, such as low concrete covers and a good corrosion resistance. Many aspects of textile reinforced concrete constructions have mostly been investigated, for example the bending and bond behavior of textile reinforced concrete members. However, there are still largely unknown fields of research such as the load case “concentrated load” in façade panels which are caused, for example, by the suspension of the panels. So far, there is no general design approach for this case and a gap in knowledge was identified. Due to an increasing application of textile reinforced concrete elements, the design of thin panels under concentrated load is of great importance.

This paper presents the results of the experimental investigations on carbon reinforced concrete members under concentrated load. In addition to the test results, first conclusions for carbon reinforced concrete members for such load cases are presented.

Keywords: Carbon reinforcement · Textile reinforced concrete · Concentrated load · Façade panel

1 Introduction

For a long time, research was conducted on grid-shaped textiles made of carbon fibre reinforced polymers (CFRP) or alkali resistant (AR-) glass in combination with concrete. In recent years, the composite material has found its way into practice and more and more projects have been realized. The applications range from strengthening of columns, beams and panels to new building components. These new building components include filigree special components such as shell structures but also bridges, sandwich elements and façade panels (Hegger 2011, Scholzen 2015, Schulze-Ardey 2019, von der Heid 2019).

One major application of the new composite material are the already mentioned façade panels. These can be produced with thicknesses of approximately 30 mm, as there is no need for a concrete cover for corrosion protection of reinforcement according to EC2 (Rempel 2015). Due to the low panel thickness, more space is available for the

thermal insulation without changing the external dimensions of the building. Thicker insulations will be necessary in the future, as the demands on the building physics properties of an exterior wall gradually increase.

As a result of the low component thickness, the required amount of concrete and at the same time the weight is reduced. However, this does not reduce CO₂ emissions, as a high strength concrete is required compared to thick reinforced concrete panels (Scope 2019). The low dead weight results in lower transport costs, more elements can be transported simultaneously. As no corrosion of the reinforcement is to be expected, a further advantage is the long service life.

An example of these façade components, which are only 30 mm thin, is the realised building project “Neuer Markt” as shown in Fig. 1, where the panel has a size of up to nine square meters.



Fig. 1. Façade panel “Neuer Markt” a) During assembly, b) View of the completed façade panels (Image source: Firmengruppe Max Bögl).

In previous approvals of façade panels, the global flexural load bearing capacity, the load-bearing capacity of embedded anchors were investigated and the bond behaviour between textile and concrete. Since the results were not transferable to other projects, the investigations had to be repeated for each project. However, mechanical equations for the calculation of the flexural load-bearing capacity could be derived from previous experimental results (Rempel 2018). The load-bearing behaviour of the embedded anchors has not yet been investigated in detail. Therefore, the load bearing behaviour of thin elements under concentrated loads should be analysed. In the further course of the research project, existing calculation models, for example Eurocode 2, will be checked for their transferability to thin components (Eurocode 2011, Eurocode 2019).

In order to reduce cracks as a result of constraint caused by the panel support, the number of anchor points should be kept as low as possible. Generally, four anchor points are installed to transfer the loads resulting of wind pressure and suction. Two of these four points additionally transfer the vertical loads resulting of dead weight. In large-sized façade panels only four anchorage points leads to high concentrated forces. Especially in thin building components this is a problem, as there is only a small embedment depth for anchors. Furthermore, cracking in the anchorage area under service loads should not occur due to aesthetic reasons.

The local load bearing behaviour, which takes place in the area of concentrated load introduction, is shown in more detail in Fig. 2.

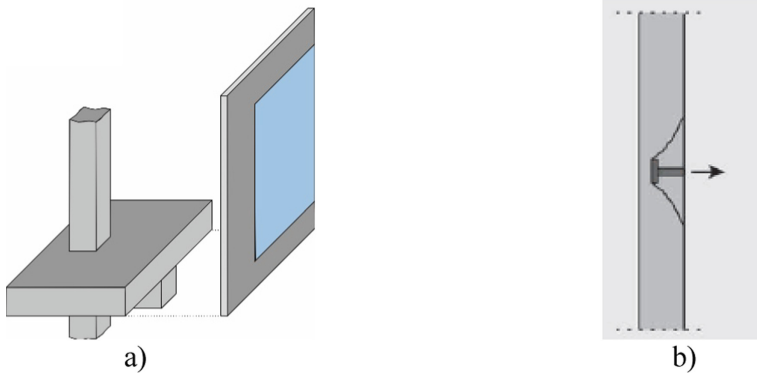


Fig. 2. Schematic drawing of concentrated load introduction a) View of façade panel, b) Side View of local bearing behaviour.

This paper presents the first test results on façade panels under concentrated tensile and compressive loads. Furthermore, the influence of a grid-shaped textile reinforcement made of CFRP will also be examined in detail and an outlook on further work is given.

2 Materials

2.1 Concrete

The concrete used meets the requirements of DIN EN 1992-1-1 (Eurocode 2 2011) and has a maximum grain size of 8 mm. A larger maximum grain size than 8 mm should not be used due to the small thickness of the panel and the mesh size of the textile. The compaction was carried out by means of a vibratory plate and no special precautions were taken for curing. In all test series the same concrete mix was used. Table 1 shows the concrete strength values of the four individual test series.

Table 1. Concrete values for tested specimen

Test serie	$f_{cm,cyl}$ (MPa)	$f_{cm,cube}$ (MPa)	$f_{cm,sp}$ (MPa)	Young modulus (MPa)
1	44.1	51.8	3.2	31.100
2	46.2	55.5	3.6	32.300
3	40.1	49.2	3.4	29.700
4	41.5	48.0	3.4	30.400

2.2 Carbon Fibre Reinforced Polymer Textile Grid

The textile reinforcement used is a planar carbon fibre reinforced polymer (CFRP) grid solidian GRID Q95/95-CCE-38 is manufactured by the company solidian GmbH. The strengths and other material properties are valid according to the manufacturer. This CFRP grid is impregnated with epoxy resin and the mesh size is 38 mm. Figure 3 shows the warp (production direction) and weft direction of the textile grid.

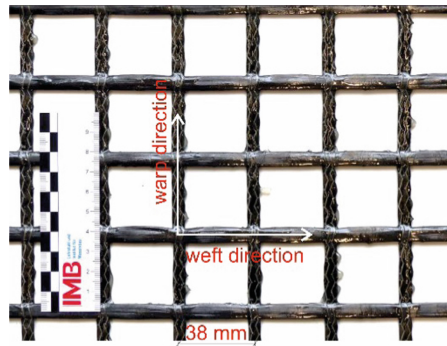


Fig. 3. Textile grid solidian GRID Q95/95-CCE-38.

2.3 Fastening Element

The tension and compression fastening element is manufactured by the company HALFEN GmbH. The fastening element is made of its stainless steel alloy and the anchoring depth is 25 mm and therefore it is suitable for use with textile concrete components. The fastening element applies to façade panels up to 30 mm thin. The fastening element has four feet which are wave-like shaped. The geometry and dimensions of the fastening element are shown in Fig. 4.

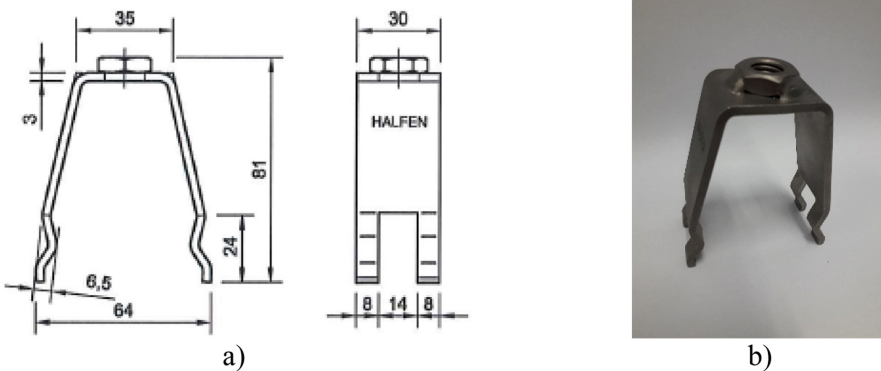


Fig. 4. a) Dimension of fastening element (DIBt 2018), b) Picture of fastening element

3 Test Setup

A total of four test series were done. Each series consists of nine single tests. To conduct all nine tests on the same panel, the dimensions of a panel (thickness $t = 30$ mm) were set $1.8 \text{ m} \times 1.8 \text{ m}$ were concreted and tested. An overview of all tests is shown in Table 2.

Table 2. Test series

Test serie	Reinforcement	Direction of loading
1	Centric	Tension
2	Centric	Compression
3	No	Tension
4	No	Compression

The panels of test serie 1 and 2 were centrally reinforced with a single layer of solidian GRID Q95/95-CCE-38 (concrete cover approx. 15 mm). The location of the fastening elements for each four panels was always identical arranged to be able to compare these experiments with each other. The nine fastening elements were distributed symmetrically on each tested panel. The outer eight fastening elements had a minimum distance to the panel edge of 0.3 m and the middle anchor was central in the middle, so the minimum distance to the panel edge was 0.9 m. The anchoring depth of every fastening element was $h_{ef} = 25$ mm.

The tested concrete panels and the position and distances of the nine fasteners to panel edges are shown in Fig. 5.

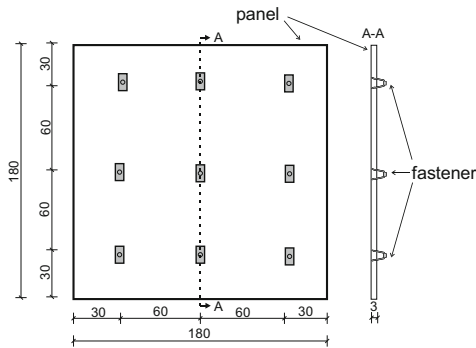


Fig. 5. Location of fastening elements.

The measurement technique and load history was the same for all four test series. The force was applied manually via a hollow piston cylinder. All tests were force-controlled.

Several load directions are known in which the concentrated load can be introduced into concrete façade panels. Figure 6 shows both load directions of the tests carried out.

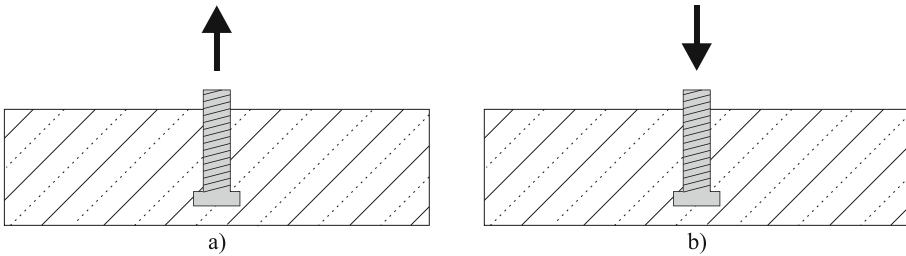


Fig. 6. Types of direction of stress a) “Tension”, b) “Compression”.

3.1 Test Setup “Tension”

The test setup in which a tension load was induced orthogonally to the panel was leaned on the test setup from Curbach (2008). A typical load situation in the real façade component is the load from wind suction, which exerts a tensile load on the fastener. In the tests, this tensile load was applied centrally to the fastening element.

The experimental setup including tripod, hollow piston cylinder, plastic ring, concrete panel and fastening elements. Moreover, there is a calotte to obtain a centric load introduction. Figure 7 shows the test setup.

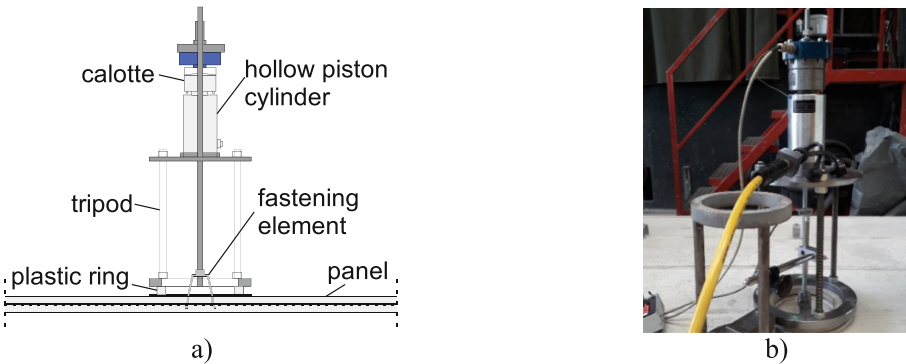


Fig. 7. Experimental test setup “Tension” a) Drawing, b) Picture.

The introduced point load is supported along a circle (plastic ring) and the selected support diameter is derived from ETAG001 (DIBt 2010) and was chosen to $d = 176 \text{ mm}$. Figure 8 shows the load direction of a centric tensile test.

3.2 Test Setup “Compression”

A typical load situation in the real façade component is the load from wind pressure, which exerts a compression load on the fastening element. The experimental setup for Compression including a stiff frame, hollow piston cylinder, plastic ring, concrete plate and fastening elements and a calotte. Figure 9 shows the test setup.

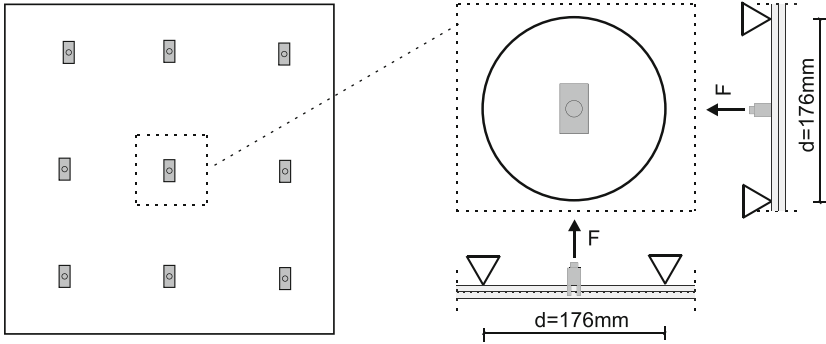


Fig. 8. Principle outline of the experimental setup with tension load direction.

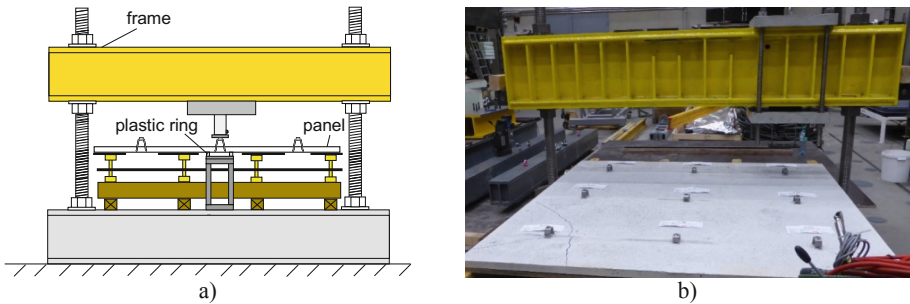


Fig. 9. Experimental test setup “Compression” a) Drawing, b) Picture.

A solid and rigid frame was required for the tests. The plastic ring for supporting the plate along a circle was aligned with screws so that it sat on the concrete panel to ensure that plastic ring was pressed against the panel. The panel was realigned for each experiment and the cylinder was moved on the steel beam of the frame. Handling the $1.8 \text{ m} \times 1.8 \text{ m}$ panel was complicated.

As well as during the tensile tests the introduced concentrated load is supported along a circle and the selected support diameter is based on ETAG001 (DIBt 2010) and was chosen to 195 mm. Figure 10 shows the load direction of a centric compression test.

4 Test Results

As described above, four series of tests were carried out, two with load direction in tension (series 1 and 3) and two in compression (series 2 and 4). The major test results are shown in Table 3. The mean load-bearing capacities include all nine tests of each series.

The mean load-bearing capacities of the Tension tests are lower than the ones with Compression. The difference in capacity between the tests with (test series 1 and 2) and without the textile reinforcement (test series 3 and 4) is neglectable for both compression and tension loads. Furthermore, for both load directions and reinforcement configurations the coefficient of variation is at most 11%.

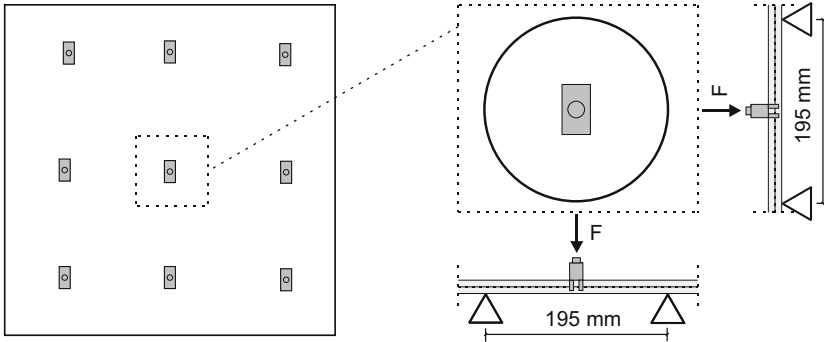


Fig. 10. Principle outline of the experimental setup.

Table 3. Maximal forces of experimental investigations.

Test series	Mean load-bearing capacity [kN]	Standard deviation [kN]	Coefficient of variation [-]	Failure
1	16,0	0,9	6%	Concrete rapture
2	27,4	1,7	6%	Concrete rapture
3	15,9	1,3	8%	Concrete rapture
4	24,8	2,8	11%	Concrete rapture
Tension (1 + 3)	16,0	1,1	7%	Concrete rapture
Compression (2 + 4)	26,1	2,3	9%	Concrete rapture

During the tension tests with CFRP reinforcement concrete rapture cones have formed. Figure 11 shows exemplary fracture patterns of these tests (test serie 1).



Fig. 11. Concrete rapture cone of a tension test with CFRP reinforcement a) side view, b) front view.

When looking at the fracture patterns, it can be seen that a rapture cone occurred but there is no splitting of the concrete panel. Figure 12a) shows exemplary fracture patterns of compression tests with reinforcement (test serie 2). Figure 12b) shows the fracture pattern of a concrete panel without reinforcement (thickness $t = 30$ mm) with dimensions $0.5 \text{ m} \times 0.5 \text{ m}$ in comparison.



Fig. 12. a) Concrete rapture cone of a compression test with CFRP reinforcement reinforced panel ($1.8 \text{ m} \times 1.8 \text{ m}$), b) Tensile test with concrete panel ($0,5 \text{ m} \times 0,5 \text{ m}$) without reinforcement.

5 Evaluation of Test Results

In addition to the failure modes of pulling out or pulling through and steel breakage of the single fastening element, a distinction can be made in fastening technology between concrete rapture and splitting in the event of centric tension (Curbach 2008).

Figure 13 shows the two failure modes which are shown in Fig. 11 and Fig. 12.

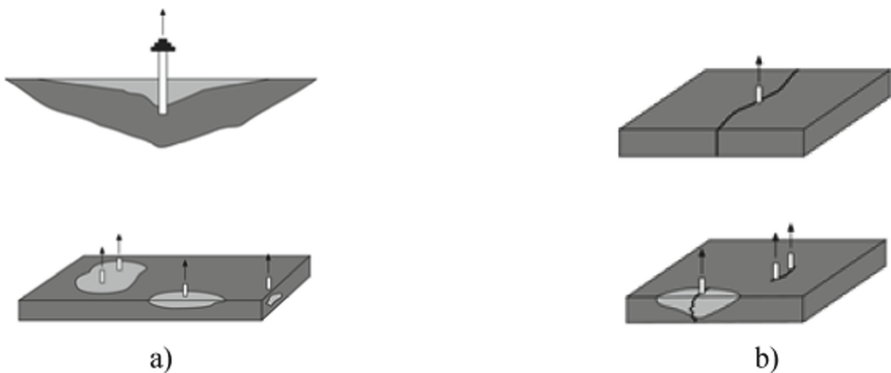


Fig. 13. a) Type of failure "Concrete Rapture", b) Type of failure "Splitting".

Various influences on the local load-bearing behaviour are well known from literature for steel reinforced concrete construction. To evaluate the fracture load and the fracture

patterns in the experimental investigations following parameters have been varied: The influence of textile reinforcement, load direction, distance to panel edge. In order to obtain a statement on the individual parameters, they will be considered separately hereinafter.

5.1 Influence of Textile Reinforcement

The test specimens were produced with a central reinforcement layer and without reinforcement respectively in order to analyse the influence of the reinforcement layer on the load-bearing behaviour. Based on the fracture patterns of the tension tests it can be seen that the textile reinforcement remained unbroken, just the concrete failed in tension.

For this reason, the tensile strengths of the concrete have to be taken into account in order to obtain a comparison between the individual test series. It can be seen that the measured failure tensile force of the test specimens with and without reinforcement does not differ greatly. Hence, it can be assumed that the textile reinforcement does not have a particularly positive or negative effect on the load bearing behaviour.

5.2 Load Direction

It is known from the literature that a different direction of loading also results in significant differences in the load-bearing behaviour (Eligehausen 2000). This circumstance can be shown particularly clearly for the types of load shown in Fig. 6, since the flow of force is different.

In the conducted tests described above, only the direction of loading in “tension” and compression” was examined. Here, a clear difference in the fracture loads is discernible. The tests with compression load have a much higher fracture load. Whereas under tensile loading a concrete rupture cone breaks out on the upper side of the panel, under compressive loading a concrete rupture cone breaks out on the underside of the panel and activates a different concrete cross-sectional area due to the different stress condition in the area of force application and the geometry of the fastener.

5.3 Distance to Panel Edge

As is known from the literature (Eligehausen 2000, Curbach 2008), the edge distance has an influence on the type of failure and thus also on the maximum value of the failure load and scatter of the failure loads. In contrast to the panels with the dimensions $0.5\text{ m} \times 0.5\text{ m}$ (Fig. 12b), the panels with the dimensions $1.8\text{ m} \times 1.8\text{ m}$ (Fig. 11) did not split in any of the tests so the decisive type of failure was concrete rupture failure.

The shortest edge distance of the fastener in the middle of the panels ($0.5\text{ m} \times 0.5\text{ m}$) had a maximum length of 0.25 m to all four sides, whereby the shortest edge distance of one of the outer four fasteners at the panel corners of the panels ($1.8\text{ m} \times 1.8\text{ m}$) to at most two sides with a length of 0.3 m was not significantly greater, whereby the edge distance to the remaining two sides was significantly greater at 1.5 m .

It is assumed that this larger edge distance has a significant influence on the type of failure and that a large edge distance to two sides, such as that which occurs in reality in the case of the façade panels mentioned at the beginning of this paper, which were realized in practice, is also the case.

6 Conclusion and Outlook

The necessity of the investigations in the field of concentrated load application results from the increased use of thin carbon concrete components and the so far insufficiently known load bearing mechanisms of concentrated load applications.

For this purpose, four series of tests were carried out on thin panels, whereby the type of reinforcement, the direction of loading and the edge distance of the fasteners were varied. During the tests, a concrete rupture in the area of concentrated load introduction was clearly visible and a difference in the load-bearing capacities could be observed depending on the direction of loading.

On the basis of the test results it can be seen that the existence of reinforcement had no significant influence on the failure load.

Furthermore, it can be seen that a significantly higher failure load occurred in the compression tests compared to the tensile tests due to different fracture surfaces of the concrete rupture cone.

Finally, no splitting effects were observed in the selected edge distances of the panel with a size of 1.8 m × 1.8 m, which is why a connection between the type of failure and the edge distance is assumed.

The variation of other parameters should be aimed at for further experiments in order to create a design model for the concentrated load transfer from textile-reinforced concrete components. Additional parameters to be varied are, for example, other material combinations, variation of the support radius of the support and a further modification of the fastener.

In the future, the load-bearing behaviour should also be analysed with numerical simulations, whereby the tests carried out can serve for validation.

Acknowledgements. The authors would like to thank the Federal Ministry of Education and Research (BMBF) for funding the project C³-V-L6 “Bemessung und bauliche Durchbildung” within the research program “C³ - Carbon Concrete Composite”. Nr 03ZZ0336A.

References

- Curbach M, Speck K (2008) Konzentrierte Lasteinleitung in dünnwandige Bauteile aus textilbewehrtem Beton. Beuth Verlag GmbH, Berlin
- DIBt (2010) ETAG 001 - Leitlinie für die europäische technische Zulassung für Metalldübel zur Verankerung im Beton. Deutsches Institut für Bautechnik, Berlin
- DIBt (2018) Allgemeine bauaufsichtliche Zulassung/Allgemeine Bauartgenehmigung Nr. Z-21.8–2067. HALFEN Fassadenplattenankersystem FPA SL30. Deutsches Institut für Bautechnik, Berlin
- Eligehausen R, Mallée R (2000) Befestigungstechnik im Beton- und Mauerwerkbau. Ernst & Sohn, Berlin
- Eurocode 2 (2011) Design of concrete structures – Part 1–1: General rules and rules for buildings; German version EN 1992–1–1:2004 + AC:2010. European Committee for Standardization, Brussels, Belgium
- Eurocode 2 (2019) Design of concrete structures – Part 4: Design of fastenings for use in concrete; German version EN 1992–4:2018. European Committee for Standardization, Brussels, Belgium

- Hegger J, Will N, Schneider M (2011) Textilbeton: Tragverhalten – Bemessung – Sicherheit. Tagungsband zum 6. Kolloquium textilbewehrten Tragwerken (CTRS6), Berlin, pp 269–284
- Rempel S (2015) Filigrane großformatige Fassadenplatte mit Carbonbewehrung für das Bauvorhaben „Neuer Markt“. Tudalit: leichter bauen – Zukunft formen, p 11
- Rempel S (2018) Zur Zuverlässigkeit der Bemessung von biegebeanspruchten Betonbauteilen mit textiler Bewehrung. Institute of Structural Concrete, RWTH Aachen University, Doctoral Thesis
- Scholzen A, Chudoba R, Hegger J (2015) Thin-walled shell structures made of textile-reinforced concrete: part I: Structural design and construction. *Struct Concr* 16(1):106–114
- Schulze-Ardey J, Bosbach S (2019) Bemessung und bauliche Durchbildung von Carbonbeton. Tagungsband der 11. Carbon- und Textilbetontage, pp 110–111
- Scope C (2019) Nachhaltigkeitsbewertung von Carbonbeton: ein Leistungsvorsprung im Vergleich. Tagungsband der 11. Carbon- und Textilbetontage, pp 88–89
- Von der Heid A, Grebe R, Will N, Hegger J (2019) Großformatige Sandwichelemente mit Deckschichten aus Textilbeton. *Beton- und Stahlbetonbau* 114:1–9